Experimental and Molecular Pathology 106 (2019) 123–130

Contents lists available at ScienceDirect

Experimental and Molecular Pathology

journal homepage: www.elsevier.com/locate/yexmp

Baicalin protects human retinal pigment epithelial cell lines against high glucose-induced cell injury by up-regulation of microRNA-145

Chunhua Dai[a,b], Shanhao Jiang[b], Cuiying Chu[b], Meng Xin[b], Xiufen Song[b], Bojun Zhao[a,*]

[a] Department of Ophthalmology, Shandong Provincial Hospital Affiliated to Shandong University, Jinan 250021, China
[b] Department of Ophthalmology, Yantai Affiliated Hospital of Binzhou Medical University, Yantai 264100, China

ARTICLE INFO

Keywords:
Diabetic retinopathy
Baicalin
MicroRNA-145
NF-κB
p38MAPK

ABSTRACT

Background: Diabetic retinopathy (DR) is a common complication of diabetes mellitus, which is a major reason of blindness. Baicalin (BAI) is a flavonoid extracted from *Scutellaria baicalensis*, whose pharmacological characterizes have been widely reported in various diseases. However, it remains unclear the effect of BAI on DR. The study aimed to confirm the protective effect of BAI on DR.

Methods: ARPE-19 cells and HRMECs were exposed to the high glucose (HG) environment to construct a cell injury model. After treatment with HG and BAI, cell viability, apoptosis, inflammatory cytokines and ROS generations were determined in ARPE-19 cells and HRMECs. Subsequently, microRNA-145 (miR-145) inhibitor and its negative control were transfected into ARPE-19 cells, and the regulatory effects on HG-and BAI-co-treated cells were detected. NF-κB and p38MAPK signaling pathways were finally examined to state the underling mechanisms.

Results: HG treatment significantly induced ARPE-19 cells and HRMECs injury *in vitro*. BAI significantly promoted cell proliferation, reduced apoptosis, as well as inhibited the release of IL-1β, IL-6, IL-8 and ROS level in HG-injured ARPE-19 cells and HRMECs. Additionally, the expression level of miR-145 was up-regulated in HG- and BAI-co-treated cells. More importantly, miR-145 inhibition reversed the protective effect of BAI on HG-injured ARPE-19 cells. Besides, we observed that BAI inhibited the activations of NF-κB and p38MAPK pathways by up-regulating miR-145.

Conclusions: Results demonstrated that BAI exhibited the protective effect against HG-induced cell injury by up-regulation of miR-145.

1. Introduction

Diabetic retinopathy (DR) is one of the most common and severe complications of diabetes mellitus (Ye et al., 2017). Due to the influence of hyperglycemia, the small blood vessels and neurons of the retina are damaged, and the normal protective function of capillaries is lost, thereby causing various fundus lesions (Gologorsky et al., 2012; Gulshan et al., 2016). Generally, the fundus lesions were appeared in diabetic patients who had diabetes at least 20 years (Lobo et al., 2001). Evidences have demonstrated that the longer a person has diabetes, the higher the risk of developing DR (Keel et al., 2014; Soni et al., 2014). With the rapid advances in medical technology, more options have been provided for the treatment of DR, such as laser surgery, vitrectomy, and vascular endothelial growth factor inhibitors (anti-VEGFs) or steroids treatment (Baker et al., 2016; Stitt et al., 2016). Despite these methods can effectively slow or prevent further vision loss caused by DR, it is still incurable. Therefore, it is urgently to explore a novel method for the treatment of DR.

Increasing evidences have demonstrated the remarkable effect of traditional Chinese medicine (TCM) for the treatment of DR (Guizhen and Ying, 2013; Zhang and Shi, 2018). An interesting research stated the protective effect of puerarin on DR (Teng et al., 2009). Additionally, other study found a curative effect of ligustrazine on non-proliferative diabetic retinopathy (NPDR) (Wang et al., 2015). Baicalin (BAI, molecular formula: $C_{21}H_{18}O_{11}$, molecular weight: 446.35) is a common TCM, which extracts from the dry roof of *Scutellaria baicalensis* (Zhou et al., 2016). The various pharmacological effects of BAI, such as anti-tumor, anti-inflammation, analgesic and anti-oxidant have been clarified in the recent studies (Ciesielska et al., 2004; Ding et al., 2016; Gao et al., 2017). It was exhibited that BAI could down-regulate the pro-

* Correspondence author at: Department of Ophthalmology, Shandong Provincial Hospital Affiliated to Shandong University, No. 324, Jingwuweiqi Road, Jinan 250021, Shandong, China.
E-mail address: zhaobojun2018@sohu.com (B. Zhao).

https://doi.org/10.1016/j.yexmp.2019.01.002
Received 8 August 2018; Received in revised form 3 January 2019; Accepted 4 January 2019
Available online 06 January 2019
0014-4800/

inflammatory mediators and cytokines of interleukin-1β (IL-1β), IL-6, tumor necrosis factor-a (TNF-a), and inhibit the activation of nuclear factor-κB (NF-κB) signaling pathway (Hsieh et al., 2007). Furthermore, BAI could prevent reactive oxygen species (ROS) production by inhibiting xanthine oxidase (Shieh et al., 2000). However, whether BAI is an effective agent for the treatment of DR is still unclear.

In the present study, we constructed high glucose (HG)-induced injury model to simulate DR *in vitro*. The effect and underling mechanism of BAI on HG-injured ARPE-19 cells and human retinal microvascular endothelial cells (HRMECs) were preliminarily investigated. The findings might provide a new idea for the treatment of DR.

2. Materials and methods

2.1. Cell culture and treatment

ARPE-19 cells obtained from American Type Culture Collection (ATCC, Rockville, MD, USA), and HRMECs purchased from Guangzhou Jennio Biotech Co., Ltd. (Guangzhou, China) were used in the present study. ARPE-19 cells and HRMECs were cultured in the complete growth medium containing Dulbecco's modified Eagle's medium/F-12 (DMEM/F-12) with 10% fetal bovine serum (FBS), 100 μg/mL streptomycin, and 100 U/mL penicillin (all from Gibco, Thermo Fisher Scientific Inc., Waltham, MA, USA). These cells were placed at 37 °C with 95% air and 5% CO_2 to incubate. Medium was renewed two or three times weekly.

For HG treatment, ARPE-19 cells were incubated in 6-well culture dishes, and the different concentrations of glucose (0, 10, 30, 50, 70 and 100 mM) were added to medium. The experiments performed in HRMECs were treated with 50 mM glucose. All these treated cells were incubated at 37 °C in a humidified chamber of 5% CO_2 for 48 h. Untreated cells stimulated with 5.5 mM glucose served as control. BAI purchased from Sigma-Aldrich (St. Louis, MO, USA) was dissolved in Dimethyl sulfoxide (DMSO, Sigma-Aldrich) and adjusted the concentrations to 2.5, 5, 10, 50 and 100 μM. ARPE-19 cells and HRMECs were treated with different concentrations of BAI for 12 h in the following experiments.

2.2. Cell viability assay

Cell Counting Kit-8 (CCK-8, Roche, Mannheim, Germany) was carried out to measure the viabilities of ARPE-19 cells and HRMECs. In brief, ARPE-19 cells and HRMECs were placed in 96-well culture plate at a density of 5×10^3 cells/well, and incubated at 37 °C with 95% air and 5% CO_2 for 24 h. Subsequently, ARPE-19 cells and HRMECs were treated with BAI and HG and further incubated for 48 h. After incubation, CCK-8 solution (10 μL/well) was added to the culture medium, and cells were incubated for 1 h at 37 °C with 95% air and 5% CO_2. The absorbance was measured at 450 nm using a Microplate Reader (Bio-Rad, Hercules, CA, USA).

2.3. Apoptosis assay

After treatment with BAI and HG, ARPE-19 cells and HRMECs were harvested and washed twice with phosphate-buffered saline (PBS, Gibco). Cell apoptosis was then examined by Annexin V-fluorescein isothiocynate (FITC)/propidium iodide (PI) apoptosis detection kit (BD Pharmingen, San Diego, CA, USA). The treated cells were re-suspended in 1 × binging buffer (Sigma-Aldrich), and 500 μL cell suspensions were added to the flow tube. Afterward, 5 μL Annexin V-FITC and 10 μL PI were supplemented in the cell suspension and stained cells for 15 min at room temperature in the dark. Flow cytometry analysis was done by using a FACS can (Beckman Coulter, Fullerton, CA, USA). Data in the experiment were analyzed by using FlowJo software (Treestar, Ashland, OR, USA).

2.4. Enzyme-linked immunosorbent assay (ELISA)

After treatment with BAI and HG, the culture supernatants from treated cells were collected from 24-well plates. Subsequently, the concentrations of pro-inflammatory cytokines of IL-1β, IL-6 and IL-8 were measured by using ELISA kits (R&D Systems, Abingdon, UK) according the protocols supplied by the manufacturer.

2.5. The intracellular ROS level assay

The intracellular ROS level in ARPE-19 cells and HRMECs co-treated with BAI and HG was measured by flow cytometry with 2, 7-dichlorofluorescein diacetate (DCFH-DA) (Nanjing Jiancheng, Nanjing, China). The treated cells were incubated with 10 μM DCFH-DA for 20 min at 37 °C under the dark conditions. Subsequently, these cells were washed with PBS for three times, and re-suspended in PBS for adjusting the concentration to 1×10^6 cells/mL. Afterward, cells were monitored by using flow cytometry at wavelengths of 488 nm excitation and 521 nm emission. ROS generation was analyzed by using FACScan flow cytometer and CellQuest software (Becton Dickinson, San Jose, CA, USA).

2.6. Cell transfection assay

The plasmids of miR-145 inhibitor (sequence: 5′-AGG GAU UCC UGG GAA AAC UGG AC-3′) and the negative control (NC, sequence: 5′-UCA CAA CCU CCU AGA AAG AGU AGA-3′) were synthesized by GenePharma Co. (Shanghai, China). After co-treatment with HG and BAI, these plasmids were transfected into ARPE-19 cells or HRMECs by using Lipofectamine 3000 reagent (Invitrogen, Carlsbad, CA, USA) according to the manufacturer's protocol.

2.7. Real-time quantitative PCR (RT-qPCR)

Total RNA was isolated from treated or transfected cells by using TRIzol reagent (Invitrogen). Reverse transcribed to cDNA was performed by using the MultiscribeRTkit and random hexamers or oligo (dT, Applied Biosystems, Foster City, CA, USA). The relative mRNA expression levels of IL-1β, IL-6 and IL-8 were analyzed by using One Step SYBR® PrimeScript®PLUS RT-RNA PCR Kit (TaKaRa Biotechnology, Dalian, China). For detection of the miR-145 expression level, miScript SYBR Green PCR Kit (Qiagen, Valencia, CA, USA) with the Stratagene Mx3000P real-time PCR system (Stratagene, La Jolla, California, USA) was performed. β-actin and U6 were used to normalize the expression levels of IL-1β, IL-6 and IL-8 and miR-145, and data were calculated by the $2^{-\Delta\Delta Ct}$ method (Livak and Schmittgen, 2012).

2.8. Western blot

ARPE-19 cells and HRMECs were collected after treatment with BAI and HG, and extracted by using RIPA lysis buffer (Beyotime Biotechnology, Shanghai, China) for 30 min at 4 °C. The BCA™ Protein Assay Kit (Pierce, Appleton, WI, USA) was used to analyze the concentration of total protein. Sodium dodecyl sulfate-polyacrylamide gel electrophoresis (SDS-PAGE) electrophoresis analysis was performed to separate the sample proteins. Subsequently, the proteins were transferred to polyvinylidene fluoride (PVDF) membranes (Millipore, Bedford, Massachusetts, USA). After blocking with 5% non-fat milk, the membranes were incubated with the primary antibodies of CyclinD1 (ab40754), p21 (ab109199), Bax (ab32503), Bcl-2 (ab182858), Procaspase-3 (ab32150), Cleaved-caspase-3 (ab32042), p-p65 (ab97726), t-p65 (ab16502), p-IκBα (ab133462), t-IκBα (ab32518), p-p38MAPK (ab47363), t-p38MAPK (ab170099) and β-actin (ab8227, Abcam, Cambridge, UK) were incubated with the membranes at 4 °C overnight, and were then further incubated with a secondary antibody of horseradish peroxidase (HRP)-conjugated goat anti-rabbit IgG (ab205718,

1:2000, Abcam) for 1 h at room temperature. The signals were visualized by using a standard enhanced chemiluminescence (ECL) Western blotting detection reagent (GE Healthcare, Braunschweig, Germany). The intensity of the bands was quantified by using ImageJ software (Bio-Rad).

2.9. Statistical analysis

The results of multiple experiments are presented as the mean ± standard deviation (SD). All statistical analyses were performed using SPSS 19.0 statistical software (SPSS Inc., Chicago, Illinois, USA). *P*-values were calculated by using a one-way analysis of variance (ANOVA). The statistical significant result was presented as $*P < .05$, $**P < .01$ or $***P < .001$.

3. Results

3.1. HG-induced ARPE-19 cells injury model was constructed in vitro

In the initial experiment, we constructed the HG-induced cells injury model in ARPE-19 cells. The increasing concentrations of glucose (0, 10, 30, 50, 70 and 100 mM) were used to expose ARPE-19 cells, and cell viability, apoptosis, inflammatory cytokines and ROS generations were assessed. Results in Fig. 1A showed that, cell viability was significantly inhibited in ARPE-19 cells after treatment with the different concentrations of glucose at 30 mM ($P < .05$), 50 mM ($P < .01$), 70 mM ($P < .01$) and 100 mM ($P < .001$). However, cell viability was increased after treatment with 10 mM glucose as compared with control group ($P < .05$). The concentration of 50 mM glucose was then selected to treat ARPE-19 cells in the following researches. Western blot assay showed that HG (50 mM) treatment notably down-regulated CyclinD1 expression and up-regulated p21 expression compared with control group ($P < .001$, Fig. 1B and C). Moreover, we observed that HG significantly induced cell apoptosis as compared with control group ($P < .001$, Fig. 1D). Meanwhile, HG treatment obviously increased Bax and Cleaved-caspase-3 expression and decreased Bcl-2 expression in ARPE-19 cells ($P < .001$, Fig. 1E and F). Additionally, results in Fig. 1G and H revealed that the mRNAs expression and the concentrations of IL-1β, IL-6 and IL-8 were significantly enhanced after treatment with HG ($P < .01$ or $P < .001$). Besides, the production of ROS was increased in HG-treated ARPE-19 cells ($P < .01$, Fig. 1I). Above data clarified that HG-induced ARPE-19 cells injury model was successfully constructed. *in vitro*

3.2. BAI protected ARPE-19 cells and HRMECs against HG-induced cell injury

Then, the effects of BAI on HG-injured ARPE-19 cells were investigated. We used the different concentrations of BAI (0, 2.5, 5, 10, 50 and 100 μM) to treat ARPE-19 cells, and cell viability was determined by CCK-8 assay. The results showed that cell viability had no obvious changed after treatment with different concentrations of BAI, indicating that BAI had no cytotoxicity on ARPE-19 cells (Fig. 2A). Subsequently, ARPE-19 cells were pre-treated with BAI (5, 10, 50 and 100 μM) for 12 h, and then incubated with HG (50 mM) for 48 h. After incubation, cell viability was determined again. In Fig. 2B, we observed that the

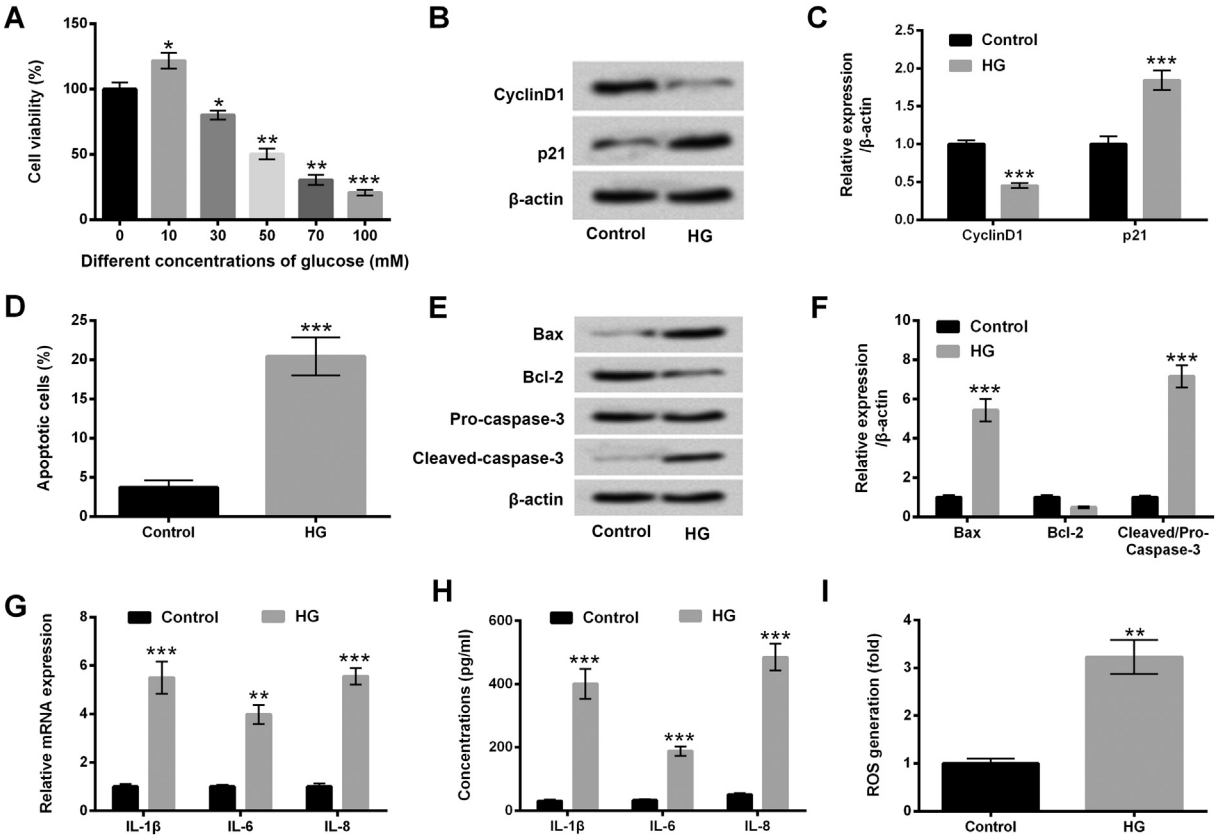

Fig. 1. HG induced ARPE-19 cells injury. Additional glucose from 0 to 100 mM was added to DMEM-F12 medium, ARPE-19 cells in the medium were incubated for 48 h. (A) CCK-8 assay was performed to determine cell viability; 50 mM was taken as HG optimum concentration to expose ARPE-19 cells. (B and C) Western blot assay was performed to examine the protein levels of CyclinD1 and p21; (D) Flow cytometry assay was performed to detect cell apoptosis; (E and F) Western blot assay was performed to examine the protein levels of Bax, Bcl-2 and Cleaved/Pro-caspase-3; (G) RT-qPCR was performed to analyze the mRNA expression levels of IL-1β, IL-6 and IL-8; (H) ELISA assay was performed to assess the concentrations of IL-1β, IL-6 and IL-8; (I) Flow cytometry with DCFH-DA was used to measure the ROS level. Data are presented as the mean ± SD of three independent experiments. *, $P < .05$; **, $P < .01$; ***, $P < .001$.

viability of ARPE-19 cells was significantly promoted after co-treatment with HG and BAI (50 and 100 μM, $P < .05$). In the following experiments, 50 μM BAI was used to stimulate ARPE-19 cells. Western blot analytical results exhibited that HG + BAI treatment remarkably increased CyclinD1 protein level and decreased p21 protein level ($P < .001$, Fig. 2C and D). Flow cytometry results stated that the percentage of apoptotic cells was significantly reduced by HG + BAI treatment ($P < .01$, Fig. 2E). The protein levels of Bax and Clevaed-caspase-3 were declined ($P < .001$) and the protein level of Bcl-2 was slightly enhanced after co-treatment with HG and BAI (Fig. 2F and G). Furthermore, results in Fig. 2H–J showed that HG + BAI treatment significantly decreased the expression levels and the concentrations of IL-1β, IL-6 and IL-8 ($P < .05$, $P < .01$ or $P < .001$), as well as inhibited the level of ROS ($P < .05$) in ARPE-19 cells. The same experiments were repeated in HRMECs, and the results are consistent with those in ARPE-19 cells ($P < .05$, $P < .01$ or $P < .001$, Supplementary Fig. 1A–J). Results indicated that BAI alleviated HG-induced cells injury in ARPE-19 cells and HRMECs, indicating the protective effect of BAI on DR.

3.3. BAI enhanced the expression level of miR-145 in HG-injured cells

In order to explore the relationship between BAI and miR-145, we measured the expression level of miR-145 in ARPE-19 cells and HRMECs after treatment with HG alone or co-treatment with HG and BAI. RT-qPCR assay results showed that HG treatment significantly down-regulated miR-145 expression in ARPE-19 cells and HRMECs ($P < .01$). But, the expression level of miR-145 was significantly up-regulated in ARPE-19 cells and HRMECs after co-treatment with HG and BAI ($P < .05$, Fig. 3A and B). To better understand the effect of miR-145 on HG-induced cell injury, the plasmid of miR-145 inhibitor was transfected into ARPE-19 cells to suppress miR-145 expression. The results in Fig. 3C revealed that miR-145 expression level was significantly decreased in miR-145 inhibitor-transfected cells, indicating good transfection efficiency ($P < .01$). Additionally, we observed that miR-145 inhibition notably down-regulated Cyclin D1, and up-regulation p21 expression in ARPE-19 cells ($P < .01$, Fig. 3D and E). The protein levels of Bax and Cleaved-caspase-3 were increased, and the protein level of Bcl-2 was decreased, as well as cell apoptosis was induced by miR-145 inhibition as compared with NC group ($P < .05$, $P < .01$ or $P < .001$, Fig. 3F–H). Further, the expression levels and the concentrations of IL-1β, IL-6 and IL-8, as well as the level of ROS were all increased by miR-145 inhibition in ARPE-19 cells ($P < .05$, $P < .01$ or $P < .001$, Fig. 3I–K). These data indicated that miR-145 might affect the protective effect of BAI on HG-injured ARPE-19 cells and HRMECs.

3.4. MiR-145 suppression reversed the protective effect of BAI on HG-injured ARPE-19 cells

Cell viability, apoptosis, inflammatory cytokines and ROS generations were assessed to study the effect of miR-145 on HG-injured ARPE-19 cells. Results showed that suppression of miR-145 significantly reversed the protective effect of BAI on HG-injured ARPE-19 cells, as inhibiting cell viability ($P < .01$, Fig. 4A), down-regulating CyclinD1 expression ($P < .001$), up-regulating p21 expression ($P < .001$, Fig. 4B and C), inducing apoptosis ($P < .01$, Fig. 4D), increasing Bax and Cleaved-caspase-3 protein levels ($P < .001$), and decreasing Bcl-2

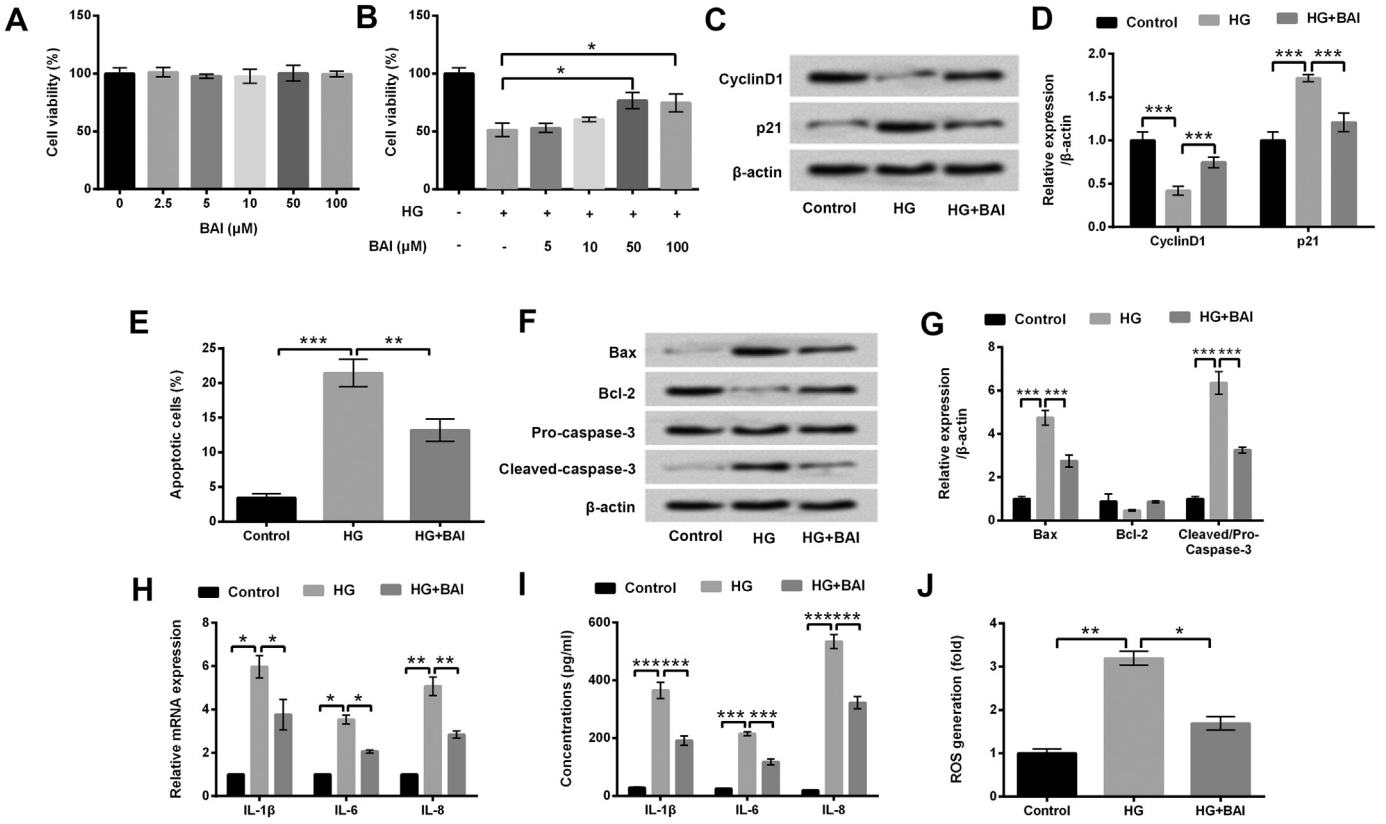

Fig. 2. BAI alleviated HG-induced cells injury in ARPE-19 cells. ARPE-19 cells were treated with the different concentrations of BAI (0, 2.5, 5, 10, 50 and 100 μM) for 12 h. (A) Cell viability was determined by using CCK-8 assay. ARPE-19 cells were pre-treated with 5, 10, 50 and 100 μM BAI and then incubated with HG (50 mM) for 48 h. (B) Cell viability was determined again. ARPE-19 cells were co-treated with BAI (50 μM) and HG (50 mM), (C and D) the protein levels of CyclinD1 and p21, (E) cell apoptosis, (F and G) the protein levels of Bax, Bcl-2 and Pro/Cleaved-caspase-3, (H) the mRNA expression levels of IL-1β, IL-6 and IL-8, (I) the concentrations of IL-1β, IL-6 and IL-8, and (J) the ROS level were analyzed by using western blot, flow cytometry, RT-qPCR, ELISA and DCFH-DA staining, respectively. Data are presented as the mean ± SD of three independent experiments. *, $P < .05$; **, $P < .01$; ***, $P < .001$.

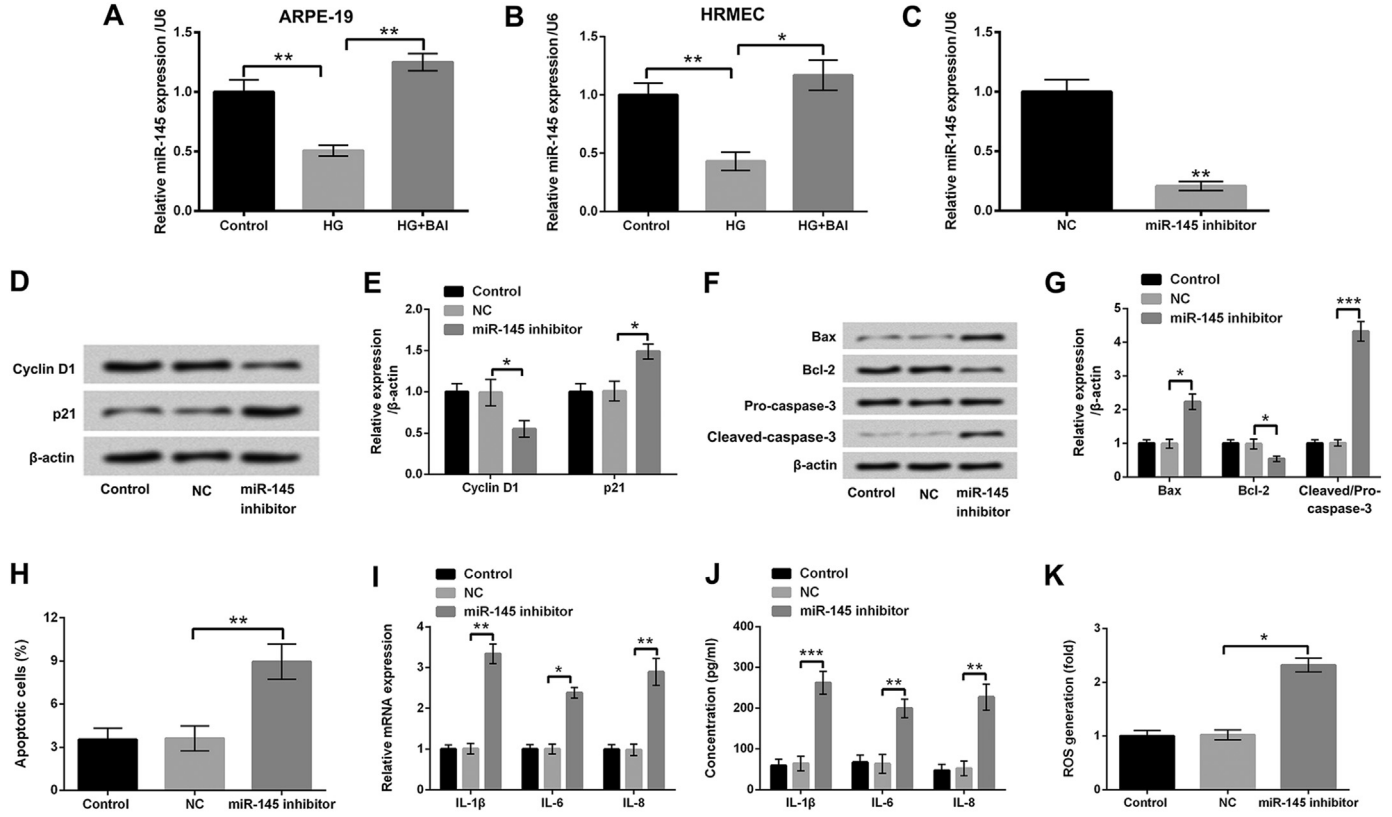

Fig. 3. BAI enhanced the expression level of miR-145 in HG-injured cells. (A and B) ARPE-19 cells and HRMECs were co-treated with BAI (50 μM) and HG (50 mM), the expression level of miR-145 was analyzed by RT-qPCR; (C) ARPE-19 cells were transfected with miR-145 inhibitor and NC, and the transfection efficiency was assessed by RT-qPCR; (D and E) the protein levels of Cyclin D1 and p21, (F and G) the protein levels of Bax, Bcl-2 and Pro/Cleaved-caspase-3, (H) cell apoptosis, (I) the mRNA expression levels of IL-1β, IL-6 and IL-8, (J) the concentrations of IL-1β, IL-6 and IL-8, and (K) the ROS level in ARPE-19 cells transfected with miR-145 inhibitor and NC were assessed by using western blot, flow cytometry, RT-qPCR, ELISA and DCFH-DA staining, respectively. Data are presented as the mean ± SD of three independent experiments. *, $P < .05$; **, $P < .01$, ***, $P < .001$.

protein level (Fig. 4E and F). Additionally, inhibition of miR-145 significantly promoted the expression levels and the concentrations of IL-1β, IL-6 and IL-8 ($P < .001$, Fig. 4G and H), as well as enhanced ROS level ($P < .01$, Fig. 4I) in HG and BAI co-treated ARPE-19 cells. The above results comprehensively illustrated that miR-145 suppression reversed the protective effect of BAI on HG-injured ARPE-19 cells.

3.5. BAI inhibited the activations of NF-κB and p38MAPK by regulating miR-145

The regulatory effect of main signaling pathways of NF-κB and p38MAPK were finally examined in the present study. The results in Fig. 5A and B displayed that HG treatment up-regulated p-p65 and p-IκBα protein levels ($P < .001$), but HG + BAI treatment obviously down-regulated p-p65 and p-IκBα protein levels ($P < .001$). However, suppression of miR-145 reversed the effect of BAI on NF-κB signaling pathway ($P < .001$). Similarly, the protein level of p-p38MAPK was up-regulated by HG ($P < .01$), and down-regulated by HG + BAI ($P < .01$). Suppression of miR-145 promoted the protein level of p-p38MAPK in HG + BAI treated cells ($P < .05$, Fig. 5C and D). Results in this experiment demonstrated that BAI blocked NF-κB and p38MAPK signaling pathways by regulating miR-145, indicating that BAI might inhibit the activations of NF-κB and p38MAPK pathways to alleviate HG-induced cell injury.

4. Discussion

DR caused by diabetes has become a serious world problem, which is a major reason leading to blindness (Papavasileiou et al., 2014). However, the effective management for the treatment of DR is still limited. The main purpose of the present study was to deduce the effect of BAI on DR *in vitro*. The cell injury model induced by HG was constructed to mimic DR. The experimental results revealed that BAI significantly inhibited HG-induced cell injury in ARPE-19 cells and HRMECs. Interestingly, we found that the expression level of miR-145 was up-regulated by BAI in HG-treated ARPE-19 cells and HRMECs, and miR-145 inhibition obviously reversed the protective effect of BAI on HG-injured cells. Finally, we found that BAI inhibited the activations of NF-κB and p38MAPK pathways *via* mediation of miR-145 expression.

Diabetes Control and Complicatuon Trial (DCCT) demonstrates that long term hyperglycemia is a direct cause of DR and other complications of diabetes (Tran et al., 2015). Several studies discovered that HG could lead to retinal pigment epithelial (RPE) cell injury and affect neovascularization and vitreous proliferation (Farnoodian et al., 2016; Mao et al., 2017). Findings from Thomas et al. indicated that HG-induced mitochondrial dysfunction and mitochondrial morphology change might play an important role in retinal muller cells loss which was associated with the occurrence of DR (Tien et al., 2017). Other study documented that HG could cause RPE cells proliferation and differentiation and functional changes (Jiang et al., 2009). Recently, HG-induced cell injury models have been widely used to mimic the process of DR, and ARPE-19 cells as a human RPE cell line, has also been widely used in many researches about DR (Coral et al., 2008; Roy et al., 2013). Study from Lin et al., used the different concentrations of glucose (1, 5, 10, 20, 50 and 100 mM) to treat ARPE-19 cells to induce cell apoptosis, and 50 mM glucose served as an optimum concentration using in this study (Lin et al., 2016). Additionally, in Yu et al. study, 50 mM glucose was used to treat ARPE-19 cells to induce diabetic

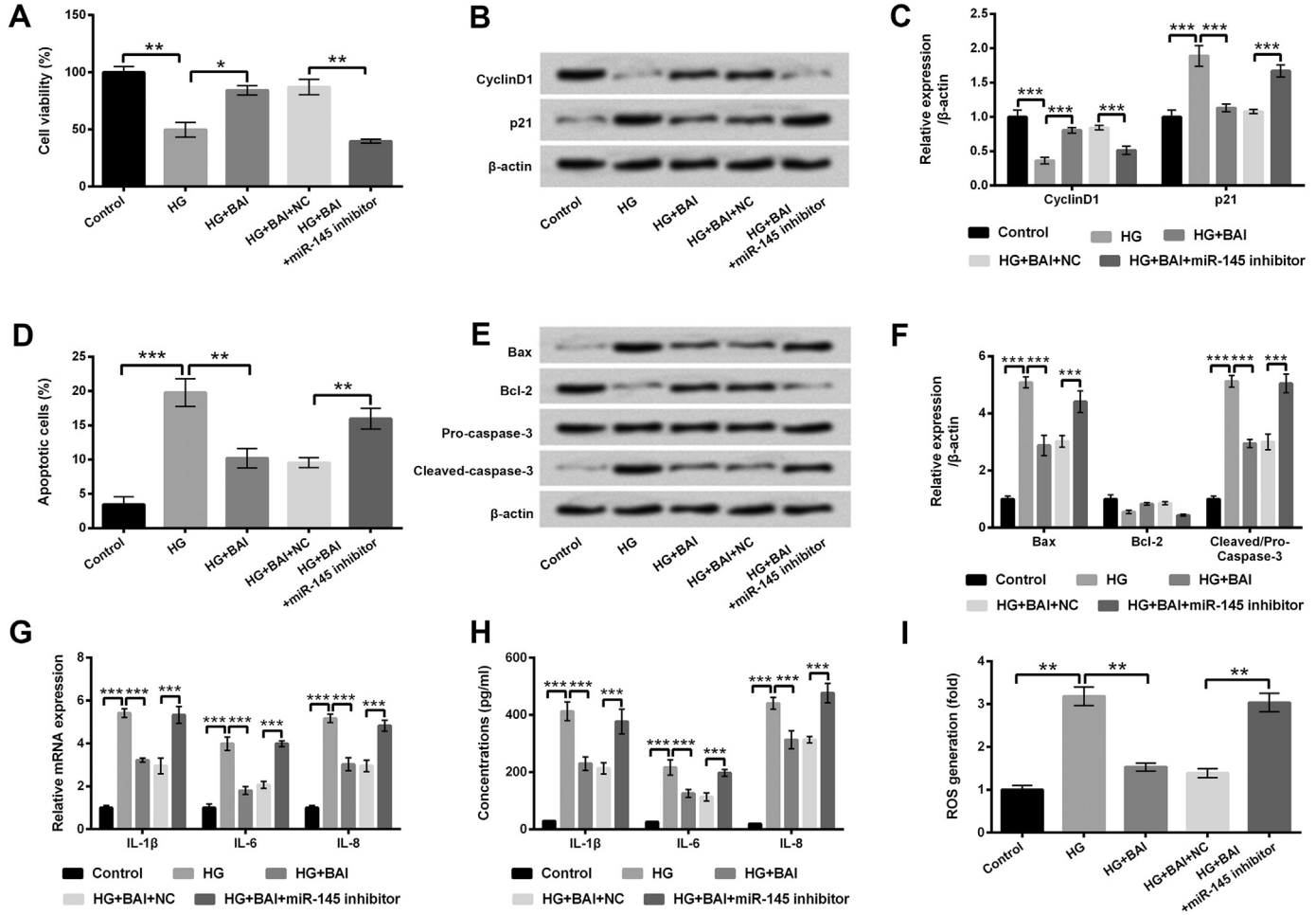

Fig. 4. BAI protected ARPE-19 cells against HG-induced cells injury by up-regulation of miR-145. ARPE-19 cells were treated with HG (50 mM), BAI (50 μM), HG (50 mM) + BAI (50 μM) and HG (50 mM) + BAI (50 μM) + miR-145 inhibitor. (A) Cell viability, (B and C) the protein levels of CyclinD1 and p21, (D) cell apoptosis, (E and F) the protein levels of Bax, Bcl-2 and Pro/Cleaved-caspase-3, (G) the mRNA expression levels of IL-1β, IL-6 and IL-8, (H) the concentrations of IL-1β, IL-6 and IL-8, and (I) the ROS level were analyzed by using CCK-8, western blot, flow cytometry, RT-qPCR, ELISA and DCFH-DA staining, respectively. Data are presented as the mean ± SD of three independent experiments. *, $P < .05$; **, $P < .01$; ***, $P < .001$.

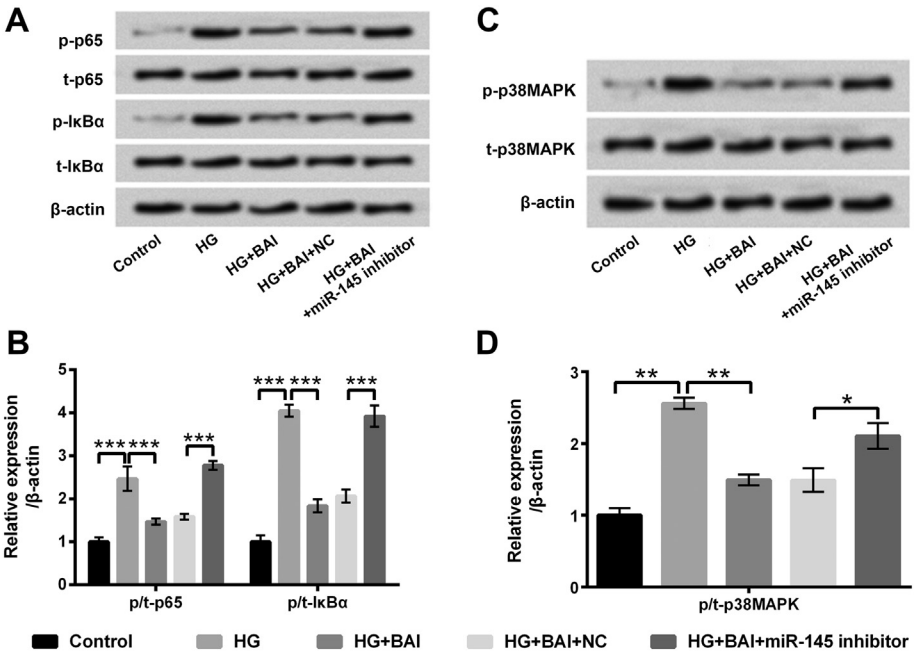

Fig. 5. BAI blocked NF-κB and p38MAPK signaling pathways by regulating miR-145. ARPE-19 cells were treated with HG (50 mM), BAI (50 μM), HG (50 mM) + BAI (50 μM) and HG (50 mM) + BAI (50 μM) + miR-145 inhibitor. The protein levels of (A and B) p/t-p65, p/t-IκBα and (C and D) p/t-p38MAPK were determined by using western blot assay. Data are presented as the mean ± SD of three independent experiments. *, $P < .05$; **, $P < .01$; ***, $P < .001$.

apoptosis *in vitro* experiments (Yu et al., 2018). Based on these studies, the different concentrations of glucose (2.5, 5, 10, 80 and 100 mM) were used to treat ARPE-19 cells to build cell injury model in the present study. We observed that HG significantly inhibited cell proliferation, induced apoptosis, increased inflammatory cytokines secretions and elevated ROS level in ARPE-19 cells. These data indicated that the ARPE-19 cells injury model induced by HG *in vitro* was successfully constructed.

As a kind of flavonoid monomer compound extracted from *Scutellaria baicalensis*, BAI has broadly applied for the comprehensive treatment of diabetes and its complications (Ku and Bae, 2015; Waisundara et al., 2011). An interesting research demonstrated the potential therapeutic effect of BAI on various ocular disorders, including DR (Xiao et al., 2014). Study from Jo et al. demonstrated that BAI could alleviate new vessel formation of retina after systemic administration, indicating that BAI might be a candidate agent for therapeutic inhibition of retinal angiogenesis (Jo et al., 2015). An important study from Jung et al. uncovered that BAI could protect retinal cells against ischemia and oxidative injuries (Jung et al., 2008). However, whether BAI exerts the protective effect on DR remains unclear. The present experiment results showed that BAI alleviated the effect of HG on cell proliferation, apoptosis, inflammatory cytokines expression and secretions and ROS level in ARPE-19 cells and HRMECs. Data indicated that BAI might protect ARPE-19 cells and HRMECs against HG-induced cell injury. These data indicated that BAI might be an effective drug for the treatment of DR.

Emerging evidence demonstrated that abnormal miRNA expression profiles in DR are closely related to the development of DR (Wu et al., 2012). Overexpression of miR-200b has been reported to prevent HG-induced increased permeability and angiogenesis in the retina in diabetes (McArthur et al., 2011). Tang et al. displayed that miR-27a could protect RPE cells against HG-induced cells injury through inhibiting inflammation and apoptosis by regulation of Toll-like receptor 4 (TLR4) (Tang et al., 2018). As intimately known that miR-145 is a tumor suppressor and plays an important role in the cellular biological processes (Sachdeva and Mo, 2010). Moreover, miR-145 has been reported in various cancers, such as renal cell carcinoma, liver cancer and colon cancer, which can inhibit tumor cells growth (Lu et al., 2014; Noh et al., 2013; Zhang et al., 2011). However, in several inflammatory injury diseases, miR-145 exerted the promoting effect on cell growth. Evidence from Zheng et al. demonstrated that miR-145 could ameliorate astrocyte injury by promoting astrocyte health and inhibiting OGD-induced apoptosis (Zheng et al., 2017). Additionally, Chen et al. demonstrated that miR-145 could alleviate HG-induced proliferation and migration in vascular smooth muscle cells by targeting ROCK1 (Chen et al., 2018). Moreover, Hui et al. reported that miR-145 could attenuate HG-induced oxidative stress and inflammation in retinal endothelial cells by regulation of TLR4/NF-κB signaling pathway (Hui and Yin, 2018). Interestingly, Su et al. revealed that Geniposide could attenuate LPS-induced injury *via* up-regulation of miR-145 in H9c2 cells (Su et al., 2018). In this study, the expression of miR-145 was down-regulated by LPS, but up-regulated by Geniposide, moreover, miR-145 inhibitor significantly reversed the protective effect of Geniposide against LPS-induced cell injury. Our results are similar to this study. The present study showed that miR-145 was up-regulated by BAI in ARPE-19 cells under the HG condition. Additionally, we found that miR-145 suppression reversed the effect of BAI on HG-treated ARPE-19 cells. These data indicated that miR-145 might play a vital role in BAI protecting ARPE-19 cells.

NF-κB and p38MAPK are important regulatory signaling pathways in the development of DR. Previous study demonstrated that NF-κB and p38MAPK signaling pathways could increase the permeability of retinal endothelial cells in DR (Adachi et al., 2012). Study from Peng et al. revealed that activation of p38MAPK might be participated in the pathogenesis of HG-related DR (Peng and Hong, 2007). In our study, we explored the regulatory effect of BAI on NF-κB and p38MAPK signaling pathways in ARPE-19 cells injured by HG. The inhibitory effects of BAI on NF-κB and p38MAPK signaling pathways were exhibited, and the regulatory mechanism might be implemented by up-regulation of miR-145 expression in HG-injured ARPE-19 cells.

5. Conclusion

In sum, the study demonstrated that BAI exerted the protective effect against HG-induced cell injury by blocking NF-κB and p38MAPK signaling pathways through up-regulation of miR-145. These findings might provide more evidence to understand the effect of BAI on the treatment of DR, and might contribute to formulate the specific treatment for DR.

Supplementary data to this article can be found online at https://doi.org/10.1016/j.yexmp.2019.01.002.

Declarations of interest

None.

Funding

This research did not receive any specific grant from funding agencies in the public, commercial, or not-for-profit sectors.

References

Adachi, T., et al., 2012. Contribution of p38 MAPK, NF-κB and glucocorticoid signaling pathways to ER stress-induced increase in retinal endothelial permeability. Arch. Biochem. Biophys. 520, 30–35.
Baker, C.W., et al., 2016. Recent advancements in diabetic retinopathy treatment from the Diabetic Retinopathy Clinical Research Network. Curr. Opin. Ophthalmol. 27, 210–216.
Chen, M., et al., 2018. MicroRNA-145 alleviates high glucose-induced proliferation and migration of vascular smooth muscle cells through targeting ROCK1. Biomed. Pharmacother. 99, 81–86.
Ciesielska, E., et al., 2004. In vitro antileukemic, antioxidant and prooxidant activities of Antoksyd S (C/E/XXI): a comparison with baicalin and baicalein. In Vivo 18, 497–503.
Coral, K., et al., 2008. Lysyl oxidase activity in proliferative diabetic retinopathy and in ARPE-19 cells exposed to glucose. Invest. Ophthalmol. Vis. Sci. 49, 3542.
Ding, X.M., et al., 2016. Baicalin exerts protective effects against lipopolysaccharide-induced acute lung injury by regulating the crosstalk between the CX3CL1-CX3CR1 axis and NF-kappaB pathway in CX3CL1-knockout mice. Int. J. Mol. Med. 37, 703–715.
Farnoodian, M., et al., 2016. High glucose promotes the pro-migratory phenotype of retinal pigment epithelial cells through increased oxidative stress. FASEB J. 30 (969.20–969.20).
Gao, C., et al., 2017. Antitumor effects of baicalin on ovarian cancer cells through induction of cell apoptosis and inhibition of cell migration in vitro. Mol. Med. Rep. 16, 8729–8734.
Gologorsky, D., et al., 2012. Therapeutic interventions against inflammatory and angiogenic mediators in proliferative diabetic retinopathy. Mediat. Inflamm. 2012, 629452.
Guizhen, L., Ying, L., 2013. Traditional chinese medicine treatment of diabetic retinopathy. J. Pract. Tradit. Chin. Intern. Med. 33, 262–267.
Gulshan, V., et al., 2016. Development and validation of a deep learning algorithm for detection of diabetic retinopathy in retinal fundus photographs. JAMA 316, 2402–2410.
Hsieh, C.-J., et al., 2007. Baicalein inhibits IL-1β- and TNF-α-induced inflammatory cytokine production from human mast cells via regulation of the NF-κB pathway. Clin. Mol. Allergy 5, 5.
Hui, Y., Yin, Y., 2018. MicroRNA-145 attenuates high glucose-induced oxidative stress and inflammation in retinal endothelial cells through regulating TLR4/NF-kappaB signaling. Life Sci. 207, 212–218.
Jiang, D., et al., 2009. Effect of hypoxia and high glucose on proliferation of retinal pigment epithelial cells and expression of VEGF and TGF-β1. Recent Adv. Ophthalmol. 29, 267–271.
Jo, H., et al., 2015. The effect of baicalin in a mouse model of retinopathy of prematurity. BMB Rep. 48, 271–276.
Jung, S.H., et al., 2008. The flavonoid baicalin counteracts ischemic and oxidative insults to retinal cells and lipid peroxidation to brain membranes. Neurochem. Int. 53, 325–337.
Keel, S., et al., 2014. Diabetes, diabetic retinopathy, and retinal vascular alterations: a systematic review. Asia Pac. J. Ophthalmol. (Phila) 3, 164–171.
Ku, S.-K., Bae, J.-S., 2015. Baicalin, baicalein and wogonin inhibits high glucose-induced vascular inflammation in vitro and in vivo. BMB Rep. 48, 519–524.
Lin, X., et al., 2016. MicroRNA-29 regulates high-glucose-induced apoptosis in human

retinal pigment epithelial cells through PTEN. In Vitro Cell Dev. Biol. Anim. 52, 419–426.
Livak, K.J., Schmittgen, T.D., 2012. Analysis of relative gene expression data using real-time quantitative PCR and the 2 −ΔΔ C T method. Methods 25, 402–408.
Lobo, C.L., et al., 2001. One-year follow-up of blood-retinal barrier and retinal thickness alterations in patients with type 2 diabetes mellitus and mild nonproliferative retinopathy. Arch. Ophthalmol. 119, 1469–1474.
Lu, R., et al., 2014. miR-145 functions as tumor suppressor and targets two oncogenes, ANGPT2 and NEDD9, in renal cell carcinoma. J. Cancer Res. Clin. Oncol. 140, 387–397.
Mao, X.B., et al., 2017. Potential suppression of the high glucose and insulin-induced retinal neovascularization by Sirtuin 3 in the human retinal endothelial cells. Biochem. Biophys. Res. Commun. 482, 341–345.
McArthur, K., et al., 2011. MicroRNA-200b regulates vascular endothelial growth factor-mediated alterations in diabetic retinopathy. Diabetes 60, 1314–1323.
Noh, J.H., et al., 2013. MiR-145 functions as a tumor suppressor by directly targeting histone deacetylase 2 in liver cancer. Cancer Lett. 335, 455–462.
Papavasileiou, E., et al., 2014. An effective programme to systematic diabetic retinopathy screening in order to reduce diabetic retinopathy blindness. Hell. J. Nucl. Med. 17 (Suppl. 1), 30–34.
Peng, H., Hong, S., 2007. Recent progress in research on the p38 MAPK cell signal pathway in diabetic retinopathy. Chin. J. Optom. Ophthalmol. 9, 139–141.
Roy, S., et al., 2013. Mitochondrial dysfunction and endoplasmic reticulum stress in diabetic retinopathy: mechanistic insights into high glucose-induced retinal cell death. Curr. Clin. Pharmacol. 8, 278–284.
Sachdeva, M., Mo, Y.Y., 2010. miR-145-mediated suppression of cell growth, invasion and metastasis. Am. J. Transl. Res. 2, 170–180.
Shieh, D.E., et al., 2000. Antioxidant and free radical scavenging effects of baicalein, baicalin and wogonin. Anticancer Res. 20, 2861–2865.
Soni, Y., et al., 2014. Effect ofaloe vera juice on diabetic and diabetic retinopathy subjects. Indian J. Life Sci. 4, 41–45.
Stitt, A.W., et al., 2016. The progress in understanding and treatment of diabetic retinopathy. Prog. Retin. Eye Res. 51, 156–186.
Su, Q., et al., 2018. Geniposide attenuates LPS-induced injury via Up-regulation of miR-145 in H9c2 cells. Inflammation 41, 1229–1237.
Tang, X., et al., 2018. MicroRNA-27a protects retinal pigment epithelial cells under high glucose conditions by targeting TLR4. Exp. Ther. Med. 16, 452–458.
Teng, Y., et al., 2009. Protective effect of puerarin on diabetic retinopathy in rats. Mol. Biol. Rep. 36, 1129.
Tien, T., et al., 2017. High glucose induces mitochondrial dysfunction in retinal muller cells: implications for diabetic retinopathy. Invest. Ophthalmol. Vis. Sci. 58, 2915–2921.
Tran, C., et al., 2015. Acute painful diabetic neuropathy: an uncommon, remittent type of acute distal small fibre neuropathy. Swiss Med. Wkly. 145, w14131.
Waisundara, V.Y., et al., 2011. Baicalin upregulates the genetic expression of antioxidant enzymes in Type-2 diabetic Goto-Kakizaki rats. Life Sci. 88, 1016–1025.
Wang, Y., et al., 2015. Effect of ligustrazine in the treatment of non proliferative diabetic retinopathy and on serum hypoxia-inducible factor-1,vascular endothelial growth factor. Chin. J. Clin. Pharmacol. 31, 1393–1395.
Wu, J.H., et al., 2012. Altered microRNA expression profiles in retinas with diabetic retinopathy. Ophthalmic Res. 47, 195–201.
Xiao, J.R., et al., 2014. Potential therapeutic effects of baicalein, baicalin, and wogonin in ocular disorders. J. Ocul. Pharmacol. Ther. 30, 605–614.
Ye, Z., et al., 2017. miRNA-1273g-3p involvement in development of diabetic retinopathy by modulating the autophagy-lysosome pathway. Med. Sci. Monit. 23, 5744–5751.
Yu, X., et al., 2018. 7,8-Dihydroxyflavone ameliorates high-glucose induced diabetic apoptosis in human retinal pigment epithelial cells by activating TrkB. Biochem. Biophys. Res. Commun. 495, 922–927.
Zhang, H., Shi, Y., 2018. Pathogenesis analysis of traditional chinese medicine on diabetic-retinopathy. J. Liaoning Univ. Tradit. Chin. Med. 20, 121–123.
Zhang, J., et al., 2011. Putative tumor suppressor miR-145 inhibits colon cancer cell growth by targeting oncogene Friend leukemia virus integration 1 gene. Cancer 117, 86–95.
Zheng, L., et al., 2017. Overexpression of microRNA-145 ameliorates astrocyte injury by targeting aquaporin 4 in cerebral ischemic stroke. Bio. Med. Res. Int. 2017.
Zhou, Y., et al., 2016. Bioactive and UV protective silk materials containing baicalin - the multifunctional plant extract from Scutellaria baicalensis Georgi. Mater. Sci. Eng. C Mater. Biol. Appl. 67, 336–344.